

Compositional stability of sediment microbial communities during a seagrass meadow decline

Marsej Markovski¹, Mirjana Najdek¹, Gerhard J. Herndl^{2,3}, and Marino Korlević^{1*}

1. Center for Marine Research, Ruđer Bošković Institute, Croatia

2. Department of Functional and Evolutionary Ecology, University of Vienna, Austria

3. Department of Marine Microbiology and Biogeochemistry, Royal Netherlands Institute for Sea
Research (NIOZ), Utrecht University, The Netherlands

*To whom correspondence should be addressed:

Marino Korlević

G. Paliaga 5, 52210 Rovinj, Croatia

Tel.: +385 52 804 768

Fax: +385 52 804 780

e-mail: marino.korlevic@irb.hr

Running title: Compositional stability of sediment communities

1 Abstract

2 The presence of seagrass shapes surface sediments and forms a specific environment for
3 diverse and abundant microbial communities. A severe decline of *Cymodocea nodosa*, a widespread
4 seagrass species in the Mediterranean Sea, has been documented. To characterise and assess
5 the changes in microbial community composition during the decline of a *Cymodocea nodosa*
6 meadow, Illumina MiSeq sequencing of the V4 region of the 16S rRNA gene was performed.
7 Samples of surface sediments from two sites, one without any vegetation and one with a declining
8 *Cymodocea nodosa* meadow, were collected at monthly intervals from July 2017 to October 2018.
9 Microbial communities were stratified by sediment depth and differed between the vegetated
10 and the nonvegetated site. Although the *Cymodocea nodosa* meadow declined to a point where
11 almost no leaves were present, no clear temporal succession in the community was observed.
12 Taxonomic analysis revealed a dominance of bacterial over archaeal sequences, with most archaeal
13 reads classified as *Nanoarchaeota*, *Thermoplasmata*, *Crenarchaeota*, and *Asgardarchaeota*.
14 The bacterial community was mainly composed of *Desulfobacterota*, *Gammaproteobacteria*,
15 *Bacteroidota*, *Chloroflexi*, *Planctomycetota*, and *Campylobacterota*. Our results show that sediment
16 microbial communities are remarkably stable and may resist major disturbances such as seagrass
17 meadow decline.

18 **Introduction**

19 Shallow coastal sediments are often colonized by seagrasses, which cover approximately 0.1
20 to 0.2 % of the global ocean (Duarte, 2002). Seagrasses penetrate the sediment with their roots and
21 rhizomes forming extensive meadows. The presence of seagrass meadows shapes surface sediments
22 and provides a specific environment for diverse and abundant microbial communities (Duarte et al.,
23 2005). Sediments colonized by seagrasses are considered hotspots for microbial activity as seagrass
24 meadows enrich the underlying sediment with organic matter (Duarte et al., 2005). High organic
25 matter content is mainly achieved by releasing dissolved organic carbon from seagrass roots and by
26 trapping organic particles from the water column (Duarte, 2002). Moreover, seagrasses stabilize the
27 underlying sediment, promoting the accumulation of organic matter and sediment particles (Fonseca
28 and Kenworthy, 1987; Terrados and Duarte, 2000; van Katwijk et al., 2010). In addition, seagrass
29 beds can also increase the availability of organic matter through the decomposition of detached
30 leaves, roots and rhizomes (Jensen et al., 2007; Liu et al., 2017).

31 Studies of marine sediment microbial communities primarily focus on changes in microbial
32 abundance and activity with sediment depth (Jørgensen and Marshall, 2016; Petro et al., 2017;
33 Starnawski et al., 2017; Orsi, 2018). Depth-dependent changes in taxonomic composition have been
34 well described differentiating surface sediment communities dominated by *Bacteria*, especially
35 *Proteobacteria*, from deeper communities characterized by *Archaea* (Orcutt et al., 2011; Chen et al.,
36 2017; Petro et al., 2017). Coastal surface sediments colonized by seagrass are not as well investigated
37 due to studies focusing primarily on rhizosphere communities and only occasionally including
38 sediment communities for comparison (Cúcio et al., 2016; Rabbani et al., 2021). Communities
39 in the rhizosphere are not species-specific and differ from those in the sediment (Cúcio et al.,
40 2016; Ettinger et al., 2017; Zhang et al., 2020). One of the main differences is the higher relative
41 abundance of *Desulfobacterota*, one of the most abundant sulphate reducing bacteria in seagrass
42 sediments, in contrast to the rhizosphere, which is characterized by *Epsilonproteobacteria* (Ettinger
43 et al., 2017). When sediment microbial communities were described, the main focus was on the

44 differences between vegetated and nonvegetated sites (Zheng et al., 2019; Sun et al., 2020). In
45 addition, these studies showed that communities differ even with respect to the meadow edge
46 (Ettinger et al., 2017). However, little is known about the response of these communities to seagrass
47 decline. As only limited information is available on the succession of microbial communities
48 in seagrass sediments it is hard to predict how and if seagrass decline influences the underlying
49 sediment communities. It was reported that the sulphate-reducing community in seagrass sediments
50 changes over time (Smith et al., 2004) and that seagrass sediment microbial communities change
51 according to nutrient availability (Guevara et al., 2014). Furthermore, seagrass restoration was also
52 found to alter the sediment microbial community (Bourque et al., 2015). These studies suggest that
53 a temporal community pattern may be observed in sediment communities of seagrass meadows and
54 that these communities could also change as a result of seagrass decline.

55 In the Mediterranean Sea, *Cymodocea nodosa* is a widespread seagrass species declining in
56 coastal areas (Ruiz Fernandez et al., 2009; Tuya et al., 2014; Orlando-Bonaca et al., 2015). The
57 rhizosphere and epiphytic communities of *C. nodosa* have been described (Cúcio et al., 2016;
58 Korlević et al., 2021a), however, little is known about sediment communities underlying *C. nodosa*
59 meadows. The aim of the present study was to characterize the taxonomic composition of sediment
60 communities of a *C. nodosa* meadow and to assess the temporal dynamics of these communities.
61 As the studied meadow experienced a major decline (Najdek et al., 2020), we investigated whether
62 this event affected the sediment microbial community structure.

63 **Materials and methods**

64 **Sampling**

65 Sediment cores were sampled in a declining *C. nodosa* meadow (vegetated site) and at an
66 adjacent area without any vegetation (nonvegetated site) both located in the Bay of Saline, east
67 coast of the northern Adriatic Sea ($45^{\circ}7'5''$ N, $13^{\circ}37'20''$ E) (Figure 1). One sediment core from
68 each site was collected monthly from July 2017 to October 2018 (Supplementary Table S1) by
69 diving using 15 cm long plastic core samplers. Sediment samples were immediately transported
70 on ice to the laboratory and stored at -80°C until further processing. A detailed description of
71 the study site, the decline of the *C. nodosa* meadow and the dynamics of environmental conditions
72 during the decline are provided in Najdek et al. (2020). Briefly, at the beginning of the study the
73 seagrass *C. nodosa* formed a large and dense meadow at the vegetated site. Seagrass roots and
74 rhizomes penetrated into slightly gravelly sandy mud, while shoots and leaves were present from
75 the southwestern coastal area up to the central part of the bay which was without any vegetation.
76 Following the regular vegetation minimum in November 2017, shoots and leaves started to decline,
77 while roots and rhizomes persisted longer. At the end of the study, after a severe meadow decline at
78 the vegetated site only very small patches persisted along the shoreline.

79 **DNA isolation**

80 Total DNA from sediment samples was extracted following a modified (Pjevac et al., 2018)
81 isolation protocol of Zhou et al. (1996). Prior to DNA isolation, cores were cut into four different
82 1 cm sections: top (0 – 1 cm), bottom (7 – 8 cm), and two middle sections: upper middle (1 – 3
83 cm) and lower middle (3 – 6 cm) section. Sediment samples were weighted (2 g) avoiding roots
84 and rhizomes from vegetated cores, mixed with 5.4 ml of extraction buffer (100 mM Tris [pH 8.0],
85 100 mM sodium EDTA [pH 8.0], 100 mM Na₃PO₄ [pH 8.0], 1.5 M NaCl, 1 % CTAB) and 10 µl

86 of proteinase K (20 mg ml⁻¹) and incubated by horizontal shaking at 225 rpm at 37°C for 30 min.
87 Thereafter 1.2 ml of 10 % SDS was added and the mixture incubated again by horizontal shaking at
88 225 rpm at 65°C for 60 min. The supernatant was collected after centrifugation at 3220 × g at room
89 temperature for 10 min and mixed with an equal volume of chloroform:isoamyl alcohol (1:1). The
90 aqueous phase was retrieved after centrifugation at 3220 × g at room temperature for 10 min. The
91 extraction procedure with the organic solvent mixture was repeated twice. After the final extraction
92 0.6 volumes of isopropanol were added to precipitate the DNA. The mixture was incubated at 22°C
93 for 60 min and centrifuged at 3220 × g at room temperature for 45 min. The obtained pellet was
94 washed twice with 10 ml of chilled 70 % ethanol, centrifuged at 3220 × g at room temperature for
95 10 min after each washing, and finally resuspended in 100 µl of deionized water.

96 Illumina 16S rRNA sequencing

97 The V4 region of the 16S rRNA gene was sequenced using a two-step PCR approach
98 described previously (Korlević et al., 2021b). Briefly, the V4 region was amplified using the 515F
99 (5'-GTGYCAGCMGCCGCGTAA-3') and 806R (5'-GGACTACNVGGTWTCTAAT-3') primers
100 from the Earth microbiome project (<https://earthmicrobiome.org/protocols-and-standards/16s/>),
101 which contained a sequence tag on the 5' end (Caporaso et al., 2011, 2012; Apprill et al., 2015;
102 Parada et al., 2016). Purified samples were sent for Illumina MiSeq sequencing (2 × 250 bp) at
103 IMGM Laboratories (Martinsried, Germany) where the second PCR of the two-step PCR approach
104 was performed using primers targeting the tag region incorporated in the first PCR. These primers
105 also contained adapter and sample-specific index sequences. For each sequencing batch, a positive
106 and a negative control were also sequenced. The positive control consisted of a mock community
107 composed of uniformly mixed DNA from 20 different bacterial strains (ATCC MSA-1002, ATCC,
108 USA), while PCR reactions without DNA template served as the negative control. Sequences
109 obtained in this study have been deposited in the European Nucleotide Archive at EMBL-EBI under
110 the accession numbers SAMEA11293274 – SAMEA11293412 and SAMEA6648825.

111 **Sequence and data analysis**

112 Sequences were analysed on the computer cluster Isabella (University Computing Centre,
113 University of Zagreb) using version 1.45.2 of mothur (Schloss et al., 2009) according to the MiSeq
114 Standard Operating Procedure (MiSeq SOP; https://mothur.org/wiki/miseq_sop/) (Kozich et al.,
115 2013) and recommendations given by the Riffomonas project (<https://riffomonas.org>) to foster data
116 reproducibility. Alignment and classification were performed using the 138.1 release of the SILVA
117 SSU Ref NR 99 database (<https://www.arb-silva.de>) (Quast et al., 2013; Yilmaz et al., 2014). A
118 cut-off of 97 % was used to cluster sequences into operational taxonomic units (OTUs).

119 Pipeline data processing and visualization were done using R (version 3.6.3) (R Core Team,
120 2020) combined with packages vegan (version 2.5.7) (Oksanen et al., 2020) tidyverse (version
121 1.3.1) (Wickham et al., 2019) and multiple other packages (Neuwirth, 2014; Xie, 2014, 2015, 2019,
122 2021a, 2021b; Xie et al., 2018, 2020; Edwards, 2020; Wilke, 2020; Allaire et al., 2021; Zhu, 2021).
123 Observed number of OTUs, Chao1, ACE, exponential of the Shannon diversity index and Inverse
124 Simpson diversity index were calculated after normalization to the minimum number of reads per
125 sample to account for different sequencing depths using vegan's function `rrarefy` (Oksanen et
126 al., 2020). Chao1 and ACE estimators were calculated using vegan's function `estimateR`, while
127 Shannon and Inverse Simpson diversity indices were obtained using vegan's function `diversity`
128 (Oksanen et al., 2020). To express both diversity indices in terms of effective number of OTUs the
129 exponential of the Shannon diversity index was retrieved (Jost, 2006). The proportions of shared
130 community members between different sediment layers and the two sites were expressed as the
131 Bray-Curtis similarity coefficient calculated on the OTU data table using vegan's function `vegdist`
132 and transformed from dissimilarities to similarities (Legendre and Legendre, 2012; Borcard et
133 al., 2018; Oksanen et al., 2020). The Principal Coordinate Analysis (PCoA) was performed on
134 Bray-Curtis dissimilarities based on OTU abundances using the function `wcmdscale` (Legendre
135 and Legendre, 2012; Oksanen et al., 2020). Differences between communities of different layers,
136 sites, years, and decay periods were tested by performing the Analysis of Similarities (ANOSIM)

137 using vegan's function `anosim` and 1000 permutations (Oksanen et al., 2020). When differences
138 between years or decay periods were tested samples were grouped based on sampling year (2017
139 and 2018) and decay of roots and rhizomes (before and after decay). The period prior to the decay
140 included samples retrieved from the begining of the study until and including February 2018, while
141 the period after the decay included samples taken after February 2018. In addition, differences
142 between richness estimators, diversity indices, and relative sequence abundances were tested by
143 performing the Mann-Whitney *U* test (function `wilcox.test`), when two groups were compared,
144 or the Kruskal-Wallis *H* test (function `kruskal.test`) followed by a pairwise comparison using
145 the Mann-Whitney *U* test (function `pairwise.wilcox.test`), when more than two groups were
146 compared. Bonferroni correction was applied to address the problem of multiple comparisons.

147 In total 3.3 million sequences were obtained after quality curation and exclusion of sequences
148 without known relatives (no relative sequences), and eukaryotic, chloroplast, and mitochondrial
149 sequences. Altogether, 68 samples from the vegetated site and 68 from the nonvegetated site
150 were analysed. The number of reads per sample ranged from 9,722 to 55,381 (Supplementary
151 Table S1). Even with the highest sequencing effort the rarefaction curves did not level off as
152 commonly observed in high-throughput 16S rRNA amplicon sequencing approaches (Supplementary
153 Figure S1, and S2). After quality curation and exclusion of sequences as mentioned above, reads
154 were clustered into 89,488 different OTUs. Normalization to the minimum number of sequences
155 (9,722) described earlier resulted in 64,335 distinct OTUs ranging from 1,774 to 3,576 OTUs per
156 sample (Supplementary Figure S3). Based on the positive control, a sequencing error rate of 0.01 %
157 was calculated which is in line with previously reported values for high-throughput sequencing data
158 (Kozich et al., 2013; Schloss et al., 2016). Following quality curation, the negative controls yielded
159 on average 34.2 ± 62.6 sequences. The detailed analysis procedure is available in a Github repository
160 (https://github.com/MicrobesRovinj/Markovski_SalineSediment16S_FrontMarSci_2022).

161 **Results**

162 To assess the richness and diversity of microbial communities in sediments of the Bay of Saline
163 the observed number of OTUs, Chao1, ACE, exponential of the Shannon diversity index, and Inverse
164 Simpson diversity index were calculated (Figure 2). The observed number of OTUs was similar
165 between the vegetated ($2,746.7 \pm 398.4$ OTUs) and the nonvegetated site ($2,883.0 \pm 353.1$ OTUs)
166 and showed no statistical difference ($p = 0.06$). Interestingly, both the highest and lowest number of
167 OTUs were observed at the vegetated site, more specifically the highest number was found in the
168 top layer ($2,976.1 \pm 262.0$ OTUs) and lowest in the bottom layer ($2,500.4 \pm 462.7$ OTUs). These
169 layers were also the only ones showing statistical difference at the vegetated site (Figure 2 and
170 Supplementary Table S2). In contrast, the observed number of OTUs at the nonvegetated site was
171 similar across sediment layers and did not show significant differences (Figure 2 and Supplementary
172 Table S3), although the lowest value was also observed in the bottom layer ($2,700.8 \pm 378.8$ OTUs).
173 During the study period, the observed number of OTUs was variable, with no clear temporal trend
174 observed (Supplementary Figure S3). Chao1, ACE, exponential of the Shannon diversity index and
175 the Inverse Simpson diversity index of sediment communities at the site with and without vegetation
176 were very similar, with no estimate or index showing a statistically significant difference (all $p > 0.1$).
177 In addition, the Chao1 and ACE richness estimators also showed no significant differences between
178 sediment layers (Figure 2 and Supplementary Tables S2 and S3). In contrast, diversity indices at
179 the vegetated site showed a difference between the top and bottom layer and between the upper
180 middle and bottom layer, with exponential of the Shannon diversity index also showing a significant
181 difference between the top and lower middle layer (Figure 2 and Supplementary Table S2). At the
182 nonvegetated site, the different sediment layers showed no statistical difference in either richness or
183 diversity (Figure 2 and Supplementary Table S3). Temporal variability in richness estimates and
184 diversity indices was high at both sites, with no clear trend (Supplementary Figures S3 and S4).

185 To evaluate the dynamics of sediment microbial communities Principal Coordinate Analyses
186 (PCoA) of Bray-Curtis distances based on OTU community data were performed. PCoA of all

samples differentiated communities based on sediment depth along the first axis, whereas samples from the vegetated and nonvegetated site were separated along the second axis (Figure 3). ANOSIM confirmed that sediment communities in the Bay of Saline differed between sediment layers with some overlap ($R = 0.48, p < 0.001$), while the communities of the vegetated and nonvegetated site showed a higher degree of overlap ($R = 0.27, p < 0.001$). When communities of different sediment layers were analysed separately, a clearer differentiation between communities of the vegetated and nonvegetated site was observed ($R = 0.45 – 0.49$, all $p < 0.001$). Interestingly, when samples from the same layer of the vegetated and nonvegetated site were compared, the top layers of the sediment showed the highest degree of similarity (Bray-Curtis, 0.64), while the lowest degree of similarity was observed in samples from the upper middle and bottom layers (Bray-Curtis, 0.59) (Figure 3 and Supplementary Figure S5). When samples from each site were analysed separately, the previously observed differentiation of samples based on sediment depth was noted (Figure 4) (ANOSIM; vegetated, $R = 0.50, p < 0.001$ and nonvegetated $R = 0.49, p < 0.001$) with the highest degree of similarity observed between samples from middle layers (Bray-Curtis; vegetated, 0.71 and nonvegetated, 0.71) and between lower middle and bottom layers (Bray-Curtis; vegetated, 0.69 and nonvegetated, 0.71) (Supplementary Figure S5). To determine whether there is a temporal succession in the community pattern, samples from each layer and site were analysed separately to exclude the effects of sediment depth and vegetation, which have been shown to primarily influence sediment community structure (Figure 4). No grouping of samples by month was observed in any of the layers and sites analysed. Although Najdek et al. (2020) described a sharp decline in aboveground biomass in the same meadow since the beginning of 2018, we did not detect a clearly defined grouping of samples based on sampling year in all the analysed layers (ANOSIM; vegetated, $R = 0.06 – 0.26, p = 0.05 – 0.18$ and nonvegetated, $R = 0.03 – 0.18 p = 0.05 – 0.29$). In addition, we also analysed the samples according to the reported decline of roots and rhizomes, as belowground biomass showed a later onset of decline than the aboveground biomass (Najdek et al., 2020). However, this analysis also did not reveal a grouping in any of the tested layers (ANOSIM; vegetated, $R = 0.07 – 0.19, p = 0.05 – 0.18$ and nonvegetated, $R = 0.16 – 0.20, p = 0.05 – 0.06$).

214 Furthermore, as with the community analysis, taxonomic classification of all samples also did not
215 indicate a temporal succession but a fairly stable community composition was detected in all layers
216 both at the vegetated and nonvegetated site (Supplementary Figure S6).

217 Archaeal sequences comprised $9.5 \pm 4.7\%$ of all reads. Sequences classified as *Archaea*
218 increased in relative abundance from the top ($4.5 \pm 1.6\%$) to the bottom sediment layer (14.1 ± 4.0
219 %). The archaeal community was comprised of *Nanoarchaeota*, *Thermoplasmatota*, *Crenarchaeota*,
220 and *Asgardarchaeota* (Figure 5). *Nanoarchaeota* comprised $3.6 \pm 1.3\%$ of all sequences and were
221 evenly distributed across the different sediment layers, whereas all other archaeal phyla showed a
222 depth-related pattern. All *Nanoarchaeota* related sequences were classified as *Woesearchaeales*,
223 with $28.2 \pm 13.5\%$ of sequences further classified as SCGC AAA011-D5. A particularly pronounced
224 depth-related pattern was found in *Thermoplasmatota*. Sequences classified as *Thermoplasmatota*
225 comprised $4.1 \pm 1.2\%$ of all sequences in the bottom sediment layer and only $0.7 \pm 0.6\%$ in the
226 top layer. The majority of sequences related to this group was further classified as Marine Benthic
227 Group D and DHVEG-1. *Crenarchaeota* comprised $1.8 \pm 2.3\%$ of all reads. This group had a
228 higher relative sequence abundance at the nonvegetated ($2.7 \pm 2.8\%$) than at the vegetated site (1.0
229 $\pm 0.9\%$) ($p < 0.0001$). The vast majority of *Crenarchaeota* related sequences were classified as
230 *Bathyarcheia*. Out of all reads, *Asgardarchaeota* comprised $0.9 \pm 0.7\%$ of sequences that could all
231 be further classified as *Lokiarchaeia*.

232 Overall, bacterial sequences ($90.5 \pm 4.7\%$) dominated over archaeal ones and were mainly
233 comprised of *Desulfobacterota*, *Gammaproteobacteria*, *Bacteroidota*, *Chloroflexi*, *Planctomycetota*,
234 and *Campylobacterota* (Figure 5). Of all reads, *Desulfobacterota* was the most abundant taxon
235 in the middle (upper middle, $19.4 \pm 2.0\%$ and lower middle, $20.2 \pm 3.2\%$) and bottom layers
236 ($18.3 \pm 3.1\%$) (Figures 5 and 6). *Desulfobacterota* consisted mainly of *Desulfosarcinaceae*,
237 *Desulfatiglandaceae*, *Desulfocapsaceae*, *Desulfobulbaceae*, and uncultured members of the
238 order *Syntrophobacterales* (Figure 6). Sequences classified as *Desulfocapsaceae* showed affinity
239 for the top sediment layer, where they comprised $26.3 \pm 8.2\%$ of *Desulfobacterota* reads

240 compared to the bottom layer where they constituted only $3.8 \pm 3.3\%$ of *Desulfobacterota* reads.
241 *Desulfosarcinaceae* and *Desulfobulbaceae* varied depending on the site. In the whole microbial
242 community, *Desulfosarcinaceae* reads were more abundant at the vegetated ($8.6 \pm 2.7\%$) than
243 nonvegetated site ($6.1 \pm 2.7\%$) ($p < 0.0001$), while sequences classified as *Desulfobulbaceae* were
244 less represented at the vegetated ($0.8 \pm 0.7\%$) than at the nonvegetated site ($1.3 \pm 0.7\%$) ($p <$
245 0.0001).

246 *Gammaproteobacteria* comprised most of the *Proteobacteria* sequences ($87.6 \pm 4.1\%$) and
247 made up the majority of all reads in the top sediment layer ($23.2 \pm 6.2\%$) (Figures 5 and 6).
248 This group was represented with more sequences at the nonvegetated ($14.8 \pm 8.9\%$) than at the
249 vegetated site ($9.5 \pm 7.4\%$) ($p < 0.001$). Out of all gammaproteobacterial sequences, 25.2 ± 8.3
250 % of reads could not be further classified than to the class *Gammaproteobacteria* (Figure 6).
251 Sequences that could be further classified were mainly assigned to *Thiotrichaceae*, B2M28,
252 *Woeseiaceae*, *Haliaceae* and *Thioalkalispiraceae* (Figure 6). The observed difference between
253 the relative abundance in *Gammaproteobacteria* at the two sites was particularly pronounced for
254 *Thioalkalispiraceae*. Sequences of this group were more abundant at the nonvegetated ($1.1 \pm 0.8\%$)
255 than at the vegetated site ($0.3 \pm 0.3\%$) ($p < 0.0001$).

256 Sequences classified as *Bacteroidota* were more abundant in the top sediment layer ($16.9 \pm$
257 2.7%) with their relative abundance decreasing with sediment depth and reaching a minimum in
258 the bottom layer ($6.7 \pm 2.2\%$) (Figures 5 and 6). A higher relative abundance of *Bacteroidota*
259 sequences was observed at the vegetated site ($12.0 \pm 4.5\%$) than at the nonvegetated site (9.8 ± 4.6
260 %) ($p < 0.01$). *Bacteroidota* were mainly composed of sequences without known relatives within
261 *Bacteroidales*, *Bacteroidetes* BD2-2, *Cyclobacteriaceae*, *Flavobacteriaceae*, *Prolixibacteraceae* and
262 *Saprospiraceae* (Figure 6). In contrast to *Bacteroidota*, sequences classified as *Chloroflexi* increased
263 with sediment depth (top layer, $4.8 \pm 2.0\%$ and bottom layer, $13.8 \pm 2.7\%$) (Figures 5 and 7).
264 *Chloroflexi* were mainly composed of *Anaerolineaceae*, while SBR1031, uncultured *Anaerolineae*,
265 sequences without known relatives within *Anaerolineae* and *Dehalococcoidia*, AB-539-J10, and

²⁶⁶ *Ktedonobacteraceae* made up the remainder of the *Chloroflexi* community (Figure 7).

²⁶⁷ *Planctomycetota* were evenly represented in the middle (upper middle, $7.3 \pm 0.9\%$ and lower
²⁶⁸ middle, $7.6 \pm 0.9\%$) and bottom layers ($7.5 \pm 1.0\%$), and less abundant in the top layer ($6.0 \pm 0.7\%$), showing no difference between the sites (vegetated, $7.0 \pm 1.2\%$ and nonvegetated, $7.1 \pm 1.0\%$) (Figures 5 and 7). The *Planctomycetota* community consisted mainly of SG8-4, *Pirellulaceae*,
²⁷⁰ 4572-13, and sequences that could not be further classified (no relative *Planctomycetota*) (Figure 7).
²⁷¹ A high proportion of *Planctomycetota* reads ($39.1 \pm 5.1\%$) were assigned to other *Planctomycetota*,
²⁷² indicating a high diversity within this group. *Campylobacterota* comprised on average $3.1 \pm 3.0\%$ of all sequences (Figures 5 and 7). Overall, no pattern related to sediment depth was observed
²⁷⁴ for this group. Slightly higher values were characteristic for the vegetated ($3.9 \pm 3.5\%$) than the
²⁷⁵ nonvegetated site ($2.3 \pm 2.3\%$) ($p < 0.001$). When differences between sites were tested for all
²⁷⁶ sediment layers, only the difference in the top layer between the two sites (vegetated, $3.4 \pm 1.8\%$
²⁷⁷ and nonvegetated, $1.5 \pm 1.6\%$) was significant ($p < 0.01$). Reads related to *Campylobacterota*
²⁷⁸ could be further classified into two families, *Sulfurimonadaceae* and *Sulfurovaceae* (Figure 7). Of
²⁷⁹ these two families, *Sulfurimonadaceae* showed an area-related difference in relative abundance.
²⁸⁰ Higher values were found at the vegetated ($2.3 \pm 3.4\%$) than at the nonvegetated site ($0.7 \pm 1.8\%$)
²⁸¹ ($p < 0.0001$). *Sulfurimonadaceae* consisted of the genus *Sulfurimonas*, while *Sulfurovaceae*
²⁸² consisted of the genus *Sulfurovum*.

284 **Discussion**

285 Sediments of seagrass meadows harbour diverse, abundant, and active microbial communities
286 (Smith et al., 2004; Duarte et al., 2005; Sun et al., 2015). Although research on microbial
287 communities of seagrass meadows mainly focused on rhizosphere communities, some studies
288 also included the underlying and surrounding sediment (Jensen et al., 2007; Cúcio et al., 2016;
289 Zhang et al., 2020). As with most sediments, a vertical structuring has been found in the microbial
290 communities of seagrass meadow sediments (Sun et al., 2020). Furthermore, a difference between
291 prokaryotic communities of seagrass meadow sediments and nonvegetated sediments has been
292 observed (Ettinger et al., 2017; Zheng et al., 2019). Temporal studies of these communities are
293 generally rare, and little is known about how microbial communities in seagrass meadow sediments
294 change with meadow decline and loss. In this study, we assessed the microbial communities in the
295 sediment of a declining *C. nodosa* meadow to gain further insights into the taxonomic composition,
296 vertical structuring, and dynamics of microbial communities in seagrass meadow sediments while
297 at the same time comparing them with bare sediments of a nearby site.

298 Shannon and Simpson indices account for both richness and evenness and are less sensitive
299 to rare taxa than richness estimators such as ACE and Chao1 (Bent and Forney, 2008). We found
300 no difference in richness (Chao1 and ACE) between sediment layers, suggesting that the observed
301 rare taxa did not play a key role in the vertical structuring of the sediment community in the Bay
302 of Saline (Figure 2). In contrast, diversity indices at the vegetated site showed a depth related
303 pattern (Figure 2). Diversity was highest in the first centimetre of the sediment and differed from
304 the deepest layer (7 – 8 cm). This is consistent with previous studies of marine sediments that
305 describe a decrease in community diversity from the surface to deeper sediment layers, even at
306 small scales within the first few meters (Petro et al., 2017; Hoshino et al., 2020). Seagrasses are
307 known to stabilize the sediment and reduce sediment resuspension (Terrados and Duarte, 2000; van
308 Katwijk et al., 2010). It is possible that the presence of the seagrass, especially roots and rhizomes,
309 increase diversity differences between the top and bottom layer by stabilizing the sediment. In

310 contrast, mechanical mixing may homogenise the sediment together with microbial cells causing
311 more similar microbial diversity in different layers. In addition, seagrass meadows increase the
312 organic matter content of the sediment through the decay of dead tissue (Jensen et al., 2007; Liu
313 et al., 2017), which may have further contributed to the observed differences between sediment
314 layers. Vertical structuring of sediment communities is typically achieved through burial, which is
315 accompanied by selection based on successive changes in environmental conditions (Petro et al.,
316 2017; Kirkpatrick et al., 2019; Marshall et al., 2019). Specific environmental conditions surrounding
317 roots and rhizomes may act as a filter during burial, separating the top from the bottom layer. In
318 contrast, the sediment of the nonvegetated site remained vertically more stable in terms of richness
319 and diversity.

320 Another component known to differentiate communities in marine sediments besides depth
321 stratification is site-specificity (Polymenakou et al., 2005; Hamdan et al., 2013), which is even
322 more pronounced in seagrass meadows where sediment microbial communities differ not only
323 between the vegetated and nonvegetated area, but also towards the edge of the seagrass patch
324 (Ettinger et al., 2017). In this study, we also observed a grouping of samples according to the
325 two sites (Figure 3), while the microbial communities of both the vegetated and nonvegetated site
326 were stratified according to sediment depth. This is in line with Sun et al. (2020) who noted that
327 the seagrass *Zostera marina* and *Zostera japonica* influence the vertical organisation of microbial
328 communities in the sediment. Although the microbial communities at the vegetated site were distinct
329 from the ones at the nonvegetated site, a high degree of overlap was present. Given that the two
330 sampling sites were in close proximity to each other, a high degree of similarity is not surprising.
331 The microbial communities in the Bay of Saline most likely originate from the same source and
332 only through burial undergo a specific selection characteristic for each site. This type of community
333 structuring (Hamdan et al., 2013; Walsh et al., 2016; Petro et al., 2019) is further supported by
334 the highest degree of similarity between the vegetated and nonvegetated site observed in the top
335 sediment layer. Also, such a high similarity of the top sediment layer may be attributed to imports of
336 seagrass detritus to the nonvegetated site. As one of the main carbon sources in *C. nodosa* meadows

(Holmer et al., 2004), seagrass detritus may easily be transported to the adjacent nonvegetated site forming similar communities in the top sediment layer. To assess the temporal dynamics of the microbial community, we analysed each sediment layer and site separately to exclude the influence of sediment depth and site-specificity. Because microbial communities of surface sediments have shorter generation times and higher biomass than communities at deeper sediment strata, and seagrass meadow sediments are hotspots for microbial activity (Duarte et al., 2005; Starnawski et al., 2017), successional changes during the decline of a seagrass meadow could be expected. Surprisingly, the decline of the *C. nodosa* meadow in the Bay of Saline appeared to have little or no effect on the microbial community, as we did not observe any grouping of communities according to month, year, or meadow condition (Figure 4). In addition, no temporal patterns were observed in the taxonomic composition, richness, or diversity of the microbial community. Such a stable community structure despite changing environmental conditions like the significant decrease of organic matter (Najdek et al., 2020) could be explained by a greater proportion of dormant or dead microbial cells remaining in the sediment, leading to a perceived taxonomic stability (Luna et al., 2002; Jones and Lennon, 2010; Cangelosi and Meschke, 2014; Carini et al., 2016; Torti et al., 2018; Bradley et al., 2019). Taxonomic identification by molecular methods such as sequencing of the 16S rRNA gene cannot distinguish between active and dormant cells, nor whether the cell is alive or dead (Cangelosi and Meschke, 2014). Indeed, it has been reported that in coastal marine sediments dead cells account for 70 % of all bacterial cells, while among living bacterial cells only 4 % grow actively (Luna et al., 2002). Furthermore, it is possible that the change in community composition may be delayed given that microbial communities in marine sediments often have very long generation times (Jørgensen and Marshall, 2016; Starnawski et al., 2017) and that some recognizable remnants of roots and rhizomes were still observed at the end of the study (Najdek et al., 2020). High metabolic versatility of microbial community members which allows functional continuity to be maintained despite changes in composition (Louca et al., 2018), may also allow for some degree of compositional stability despite changing environmental conditions. Indeed, a decoupling of microbial composition and biogeochemical processes has been observed in sediments. Bowen et al. (2011) have shown

364 that microbial communities in sediments are able to resist compositional changes despite significant
365 variations in external nutrient supply, while Marshall et al. (2021) found that the composition of
366 the nitrogen cycling community might change but these compositional changes are not reflected in
367 functional changes.

368 The archaeal community of both sites was comprised of *Nanoarchaeota*, *Thermoplasmatota*,
369 *Crenarchaeota* and *Asgardarchaeota* which are all typical sediment members (Zheng et al., 2019;
370 Sun et al., 2020). We found a nearly threefold increase in the relative abundance of *Archaea* in the
371 deepest sediment layer compared to the top layer (Figure 5). This is not surprising as it has been well
372 documented that *Bacteria* dominate the upper sediment layers while at deeper layers the distribution
373 between *Bacteria* and *Archaea* is more uniform (Chen et al., 2017). A particularly pronounced
374 increase in relative abundance with depth was observed for *Thermoplasmatota* at both sites. It is
375 possible that oxygen penetration in the uppermost sediment layer caused such a pronounced change
376 as representatives of the Marine Benthic Group D and DHVEG-1, accounting for the majority of
377 sequences within the phylum *Thermoplasmatota* (Rinke et al., 2019), are known to be restricted to
378 anoxic environments (Lloyd et al., 2013).

379 The main difference between the archaeal community of the vegetated and nonvegetated
380 site was the increased presence of *Crenarchaeota* in the nonvegetated sediment (Figure 5). This
381 difference resulted from a much greater increase in the relative abundance of *Bathyarcheia* with
382 increasing depth at the nonvegetated site (Figure 5). In a study comparing archaeal communities
383 in the sediment of a *Zostera marina* meadow with those of bare sediment, a higher presence of
384 *Bathyarchaeota* was found in the vegetated sediment, which is not consistent with our results
385 (Zheng et al., 2019). This discrepancy could have been caused by patchiness and different sampling
386 strategies. In contrast to the three samples per vegetated and nonvegetated sediment in the study of
387 Zheng et al. (2019), we analysed sixty-eight samples from each site. *Bathyarcheia*, formerly known
388 as the Miscellaneous Crenarchaeotal Group (MCG), are typically present in deeper sediment layers
389 as they are well adapted to energy limitation (Kubo et al., 2012). Since seagrasses are known to

390 directly and indirectly enrich the underlying sediment with organic matter (Terrados and Duarte,
391 2000; Duarte, 2002; Duarte et al., 2005; Jensen et al., 2007; van Katwijk et al., 2010; Liu et al.,
392 2017), it is possible that the presence of *C. nodosa* caused the observed lower relative abundance of
393 this group in the sediment at the vegetated site.

394 The sediment bacterial community of both sites consisted of taxonomic groups commonly
395 found in marine sediments such as *Desulfobacterota*, *Gammaproteobacteria*, *Bacteroidota*,
396 *Chloroflexi*, and *Planctomycetota* (Walsh et al., 2016; Hoshino et al., 2020), along with
397 *Campylobacterota*, characteristic of seagrass meadows (Jensen et al., 2007). These major groups
398 showed different patterns in relative abundance depending on sediment depth (Figures 6 and
399 7). The proportion of *Gammaproteobacteria* and *Bacteroidota* decreased with sediment depth,
400 while the relative abundance of *Chloroflexi* increased (Figure 6). Although the proportion of
401 *Desulfobacterota* remained similar in all sediment layers, *Desulfocapsaceae*, a major constituent of
402 the *Desulfobacterota* community, decreased with sediment depth (Figure 6). *Gammaproteobacteria*
403 and *Desulfobacterota* (formerly known as *Deltaproteobacteria*), were reported to decrease with
404 sediment depth, while *Chloroflexi* increased (Petro et al., 2017). Also, Smith et al. (2004)
405 documented no vertical trend in sulphate-reducing prokaryotes (*Desulfobacterota*) over a similarly
406 small depth range. Reduction of sulphate is one of many processes that affects pH in sediments,
407 while oxygen penetration controls the depth of pH minima (Silburn et al., 2017). Because
408 *Desulfocapsaceae* are neutrophilic (Galushko and Kuever, 2021) it is possible that depletion of
409 oxygen below the first centimetre and an increase in hydrogen sulphide with sediment depth
410 (Najdek et al., 2020) contributed to the observed vertical trend of this group. The pronounced
411 decline in *Gammaproteobacteria* after the top centimetre could also be attributed to the oxygen
412 penetration depth observed in the Bay of Saline (Najdek et al., 2020) coinciding with the abrupt
413 change in the relative abundance of this class. Oxygen availability could also influence the vertical
414 distribution of *Chloroflexi* and *Planctomycetota* (Figure 7), as these phyla are known to be prevalent
415 in anoxic sediments (Hoshino et al., 2020). In addition to oxygen availability, the decline of
416 *Gammaproteobacteria* and *Bacteroidota* with sediment depth may also be related to the lower

417 availability of fresh organic matter in deeper layers (Middelburg, 1989), as both of these groups are
418 known to break down and assimilate fresh detritus in coastal sediments (Gihring et al., 2009).

419 The differences in taxonomic composition of microbial communities from the vegetated
420 and nonvegetated site were not as pronounced as those influenced by sediment depth.
421 *Gammaproteobacteria* made up a large proportion of the microbial community at the nonvegetated
422 site, and as with vertical structuring, their higher presence at this site could be explained by oxygen
423 availability. This class contains representatives with a wide range of metabolisms, including
424 aerobic species (Gutierrez, 2019), which could benefit from the higher oxygen availability at
425 the nonvegetated site (Najdek et al., 2020). Indeed, a study by Ettinger et al. (2017) also found
426 a higher presence of *Gammaproteobacteria* in the sediment outside a seagrass meadow. The
427 most pronounced difference in the taxonomic composition of this class between the vegetated
428 and nonvegetated site is the higher relative abundance of *Thioalkalipiraceae* in the nonvegetated
429 sediment (Figure 6). This higher relative abundance could be due to differences in organic matter
430 content. In fact, *Thioalkalipiraceae* are known to be chemolithoautotrophs (Mori et al., 2011; Mori
431 and Suzuki, 2014) and thus may rely on inorganic compounds rather than organic matter supplied by
432 the seagrass. Slight differences were also observed in the *Desulfobacterota* community between the
433 vegetated and nonvegetated site. *Desulfosarcinaceae* were more pronounced at the vegetated site,
434 while *Desulfobulbaceae* were more pronounced at the nonvegetated site (Figure 6). Although both
435 families have been associated with the rhizosphere of seagrasses (Cúcio et al., 2016), our results are
436 consistent with previous studies that reported a high presence of *Desulfosarcinaceae* in vegetated
437 sediments and higher relative abundances of *Desulfobulbaceae* in the nonvegetated sediment (Smith
438 et al., 2004; García-Martínez et al., 2009). The most abundant *Desulfobacterota* family at both
439 the vegetated and nonvegetated site was *Desulfosarcinaceae*. The high metabolic versatility of
440 this group (Watanabe et al., 2020) may have lead to its even greater proliferation at the vegetated
441 site (Figure 6) where high concentrations of different carbon substrates may become available
442 during decomposition of organic matter. In contrast to *Gammaproteobacteria* and *Desulfobacterota*,
443 a higher relative abundance of *Bacteroidota* at the vegetated site may be influenced by the

presence of the plant itself. Seagrass cell walls contain polysaccharides like cellulose (Pfeifer and Classen, 2020) and *Bacteroidota* have been identified as decomposers of macromolecules such as cellulose (Thomas et al., 2011). The differences between the vegetated and nonvegetated sediment communities were also reflected in the higher proportion of *Campylobacterota* related sequences at the vegetated site. *Campylobacterota*, formerly known as *Epsilonproteobacteria*, are known to be closely associated with roots and rhizomes of seagrasses, particularly *Sulfurimonadaceae* (Jensen et al., 2007). In this study, the family *Sulfurimonadaceae* also contributed highly to *Campylobacterota* at the vegetated site (Figure 7). This high contribution may be caused by close proximity of the sampled sediment to roots and rhizomes. The seagrass selects the rhizosphere microbial community from the surrounding bulk sediment by enrichment of certain taxa and depletion of others (Cúcio et al., 2016; Zhang et al., 2020, 2022). It may be possible that roots and rhizomes to some degree also alter the composition of the community in the surrounding sediment in their close proximity forming the observed structure of *Campylobacterota* in our samples.

Taken together, sediment microbial communities in the Bay of Saline were depth stratified, and differed between the vegetated and nonvegetated site, however, remained temporally stable. Although the *C. nodosa* meadow experienced a sharp decline during the investigation period, no pronounced change in the microbial community was observed. The characterization of the sediment microbial community of the declining *C. nodosa* meadow in the Bay of Saline forms the basis for further studies based on methods that can differentiate active communities or methods that can provide insight into the prevailing metabolic processes during the period of seagrass decline.

⁴⁶⁴ **Acknowledgements**

⁴⁶⁵ This study was funded by the Croatian Science Foundation through the MICRO-SEAGRASS
⁴⁶⁶ project (project number IP-2016-06-7118). GJH was supported by the Austrian Science Fund
⁴⁶⁷ (FWF) through the ARTEMIS project (project number P28781-B21). We would like to thank the
⁴⁶⁸ University Computing Centre of the University of Zagreb for access to the computer cluster Isabella,
⁴⁶⁹ Margareta Buterer for technical support and Paolo Paliaga for help during sampling.

470 **References**

- 471 Allaire, J. J., Xie, Y., McPherson, J., Luraschi, J., Ushey, K., Atkins, A., et al. (2021).
- 472 *rmarkdown: Dynamic documents for R.*
- 473 Apprill, A., McNally, S., Parsons, R., and Weber, L. (2015). Minor revision to V4 region SSU
- 474 rRNA 806R gene primer greatly increases detection of SAR11 bacterioplankton. *Aquat. Microb. Ecol.* 75, 129–137. doi:10.3354/ame01753.
- 476 Bent, S. J., and Forney, L. J. (2008). The tragedy of the uncommon: Understanding limitations
- 477 in the analysis of microbial diversity. *ISME J.* 2, 689–695. doi:10.1038/ismej.2008.44.
- 478 Borcard, D., Gillet, F., and Legendre, P. (2018). *Numerical ecology with R*. 2nd ed. New York:
- 479 Springer-Verlag doi:10.1007/978-3-319-71404-2.
- 480 Bourque, A. S., Vega-Thurber, R., and Fourqurean, J. W. (2015). Microbial community
- 481 structure and dynamics in restored subtropical seagrass sediments. *Aquat. Microb. Ecol.* 74, 43–57.
- 482 doi:10.3354/ame01725.
- 483 Bowen, J. L., Ward, B. B., Morrison, H. G., Hobbie, J. E., Valiela, I., Deegan, L. A., et al.
- 484 (2011). Microbial community composition in sediments resists perturbation by nutrient enrichment.
- 485 *ISME J.* 5, 1540–1548. doi:10.1038/ismej.2011.22.
- 486 Bradley, J. A., Amend, J. P., and LaRowe, D. E. (2019). Survival of the fewest: Microbial
- 487 dormancy and maintenance in marine sediments through deep time. *Geobiology* 17, 43–59.
- 488 doi:10.1111/gbi.12313.
- 489 Cangelosi, G. A., and Meschke, J. S. (2014). Dead or alive: Molecular assessment of microbial
- 490 viability. *Appl. Environ. Microbiol.* 80, 5884–5891. doi:10.1128/AEM.01763-14.

- 491 Caporaso, J. G., Lauber, C. L., Walters, W. A., Berg-Lyons, D., Huntley, J., Fierer, N., et al.
492 (2012). Ultra-high-throughput microbial community analysis on the Illumina HiSeq and MiSeq
493 platforms. *ISME J.* 6, 1621–1624. doi:10.1038/ismej.2012.8.
- 494 Caporaso, J. G., Lauber, C. L., Walters, W. A., Berg-Lyons, D., Lozupone, C. A., Turnbaugh,
495 P. J., et al. (2011). Global patterns of 16S rRNA diversity at a depth of millions of sequences per
496 sample. *Proc. Natl. Acad. Sci. U.S.A.* 108, 4516–4522. doi:10.1073/pnas.1000080107.
- 497 Carini, P., Marsden, P. J., Leff, J. W., Morgan, E. E., Strickland, M. S., and Fierer, N. (2016).
498 Relic DNA is abundant in soil and obscures estimates of soil microbial diversity. *Nat. Microbiol.* 2,
499 16242. doi:10.1038/nmicrobiol.2016.242.
- 500 Chen, X., Andersen, T. J., Morono, Y., Inagaki, F., Jørgensen, B. B., and Lever, M. A. (2017).
501 Bioturbation as a key driver behind the dominance of bacteria over archaea in near-surface sediment.
502 *Sci. Rep.* 7, 2400. doi:10.1038/s41598-017-02295-x.
- 503 Cúcio, C., Engelen, A. H., Costa, R., and Muyzer, G. (2016). Rhizosphere microbiomes of
504 european seagrasses are selected by the plant, but are not species specific. *Front. Microbiol.* 7, 440.
505 doi:10.3389/fmicb.2016.00440.
- 506 Duarte, C. (2002). The future of seagrass meadows. *Environ. Conserv.* 29, 192–206.
507 doi:10.1017/S0376892902000127.
- 508 Duarte, C. M., Holmer, M., and Marbà, N. (2005). “Plant microbe interactions in seagrass
509 meadows,” in *Interactions between macro- and microorganisms in marine sediments*, eds. E.
510 Kristensen, R. R. Haese, and J. E. Kostka (Washington: American Geophysical Union), 31–60.
511 doi:10.1029/CE060p0031.
- 512 Edwards, M. S. (2020). *lemon: Freshing up your 'ggplot2' plots.*

- 513 Ettinger, C. L., Voerman, S. E., Lang, J. M., Stachowicz, J. J., and Eisen, J. A. (2017).
- 514 Microbial communities in sediment from *Zostera marina* patches, but not the *Z. marina* leaf or root
- 515 microbiomes, vary in relation to distance from patch edge. *PeerJ* 5, e3246. doi:10.7717/peerj.3246.
- 516 Fonseca, M. S., and Kenworthy, W. J. (1987). Effects of current on photosynthesis and
- 517 distribution of seagrasses. *Aquat. Bot.* 27, 59–78. doi:10.1016/0304-3770(87)90086-6.
- 518 Galushko, A., and Kuever, J. (2021). “*Desulfocapsaceae*,” in *Bergey’s manual of systematics*
- 519 *of Archaea and Bacteria*, ed. W. B. Whitman (online: John Wiley & Sons, in association with
- 520 Bergey’s manual trust), 1–6. doi:10.1002/9781118960608.fbm00332.
- 521 García-Martínez, M., López-López, A., Calleja, M. L., Marbà, N., and Duarte, C. M. (2009).
- 522 Bacterial community dynamics in a seagrass (*Posidonia oceanica*) meadow sediment. *Estuaries*
- 523 *Coasts* 32, 276–286. doi:10.1007/s12237-008-9115-y.
- 524 Gihring, T. M., Humphrys, M., Mills, H. J., Huette, M., and Kostka, J. E. (2009). Identification
- 525 of phytodetritus-degrading microbial communities in sublittoral Gulf of Mexico sands. *Limnol.*
- 526 *Oceanogr.* 54, 1073–1083. doi:10.4319/lo.2009.54.4.1073.
- 527 Guevara, R., Ikenaga, M., Dean, A. L., Pisani, C., and Boyer, J. N. (2014). Changes in
- 528 sediment bacterial community in response to long-term nutrient enrichment in a subtropical
- 529 seagrass-dominated estuary. *Microb. Ecol.* 68, 427–440. doi:10.1007/s00248-014-0418-1.
- 530 Gutierrez, T. (2019). “Marine, aerobic hydrocarbon-degrading *Gammaproteobacteria*:
- 531 Overview,” in *Taxonomy, genomics and ecophysiology of hydrocarbon-degrading microbes*, ed. T. J.
- 532 McGenity (Cham: Springer-Verlag), 143–152. doi:10.1007/978-3-030-14796-9_22.
- 533 Hamdan, L. J., Coffin, R. B., Sikaroodi, M., Greinert, J., Treude, T., and Gillevet, P. M.
- 534 (2013). Ocean currents shape the microbiome of Arctic marine sediments. *ISME J.* 7, 685–696.
- 535 doi:10.1038/ismej.2012.143.

536 Holmer, M., Duarte, C. M., Boschker, H. T. S., and Barrón, C. (2004). Carbon cycling and
537 bacterial carbon sources in pristine and impacted Mediterranean seagrass sediments. *Aquat. Microb.*
538 *Ecol.* 36, 227–237. doi:10.3354/ame036227.

539 Hoshino, T., Doi, H., Uramoto, G.-I., Wörmer, L., Adhikari, R. R., Xiao, N., et al. (2020).
540 Global diversity of microbial communities in marine sediment. *Proc. Natl. Acad. Sci. U.S.A.* 117,
541 27587–27597. doi:10.1073/pnas.1919139117.

542 Jensen, S. I., Kühl, M., and Priemé, A. (2007). Different bacterial communities associated with
543 the roots and bulk sediment of the seagrass *Zostera marina*. *FEMS Microbiol. Ecol.* 62, 108–117.
544 doi:10.1111/j.1574-6941.2007.00373.x.

545 Jones, S. E., and Lennon, J. T. (2010). Dormancy contributes to the maintenance of microbial
546 diversity. *Proc. Natl. Acad. Sci. U.S.A.* 107, 5881–5886. doi:10.1073/pnas.0912765107.

547 Jost, L. (2006). Entropy and diversity. *Oikos* 113, 363–375.
548 doi:10.1111/j.2006.0030-1299.14714.x.

549 Jørgensen, B. B., and Marshall, I. P. (2016). Slow microbial life in the seabed. *Annu. Rev. Mar.*
550 *Sci.* 8, 311–332. doi:10.1146/annurev-marine-010814-015535.

551 Kirkpatrick, J. B., Walsh, E. A., and D’Hondt, S. (2019). Microbial selection and survival in
552 subseafloor sediment. *Front. Microbiol.* 10, 956. doi:10.3389/fmicb.2019.00956.

553 Korlević, M., Markovski, M., Zhao, Z., Herndl, G. J., and Najdek, M. (2021a). Seasonal
554 dynamics of epiphytic microbial communities on marine macrophyte surfaces. *Front. Microbiol.*
555 12, 2528. doi:10.3389/fmicb.2021.671342.

556 Korlević, M., Markovski, M., Zhao, Z., Herndl, G. J., and Najdek, M. (2021b). Selective
557 DNA and protein isolation from marine macrophyte surfaces. *Front. Microbiol.* 12, 665999.
558 doi:10.3389/fmicb.2021.665999.

- 559 Kozich, J. J., Westcott, S. L., Baxter, N. T., Highlander, S. K., and Schloss, P. D. (2013).
560 Development of a dual-index sequencing strategy and curation pipeline for analyzing amplicon
561 sequence data on the MiSeq Illumina sequencing platform. *Appl. Environ. Microbiol.* 79,
562 5112–5120. doi:10.1128/AEM.01043-13.
- 563 Kubo, K., Lloyd, K. G., F Biddle, J., Amann, R., Teske, A., and Knittel, K. (2012). *Archaea* of
564 the Miscellaneous Crenarchaeotal Group are abundant, diverse and widespread in marine sediments.
565 *ISME J.* 6, 1949–1965. doi:10.1038/ismej.2012.37.
- 566 Legendre, P., and Legendre, L. (2012). *Numerical ecology*. 3rd ed. Amsterdam: Elsevier.
- 567 Liu, S., Jiang, Z., Deng, Y., Wu, Y., Zhao, C., Zhang, J., et al. (2017). Effects of seagrass leaf
568 litter decomposition on sediment organic carbon composition and the key transformation processes.
569 *Sci. China Earth Sci.* 60, 2108–2117. doi:10.1007/s11430-017-9147-4.
- 570 Lloyd, K. G., Schreiber, L., Petersen, D. G., Kjeldsen, K. U., Lever, M. A., Steen, A. D., et al.
571 (2013). Predominant archaea in marine sediments degrade detrital proteins. *Nature* 496, 215–218.
572 doi:10.1038/nature12033.
- 573 Louca, S., Polz, M. F., Mazel, F., Albright, M. B. N., Huber, J. A., O'Connor, M. I., et al.
574 (2018). Function and functional redundancy in microbial systems. *Nat. Ecol. Evol.* 2, 936–943.
575 doi:10.1038/s41559-018-0519-1.
- 576 Luna, G. M., Manini, E., and Danovaro, R. (2002). Large fraction of dead and inactive bacteria
577 in coastal marine sediments: Comparison of protocols for determination and ecological significance.
578 *Appl. Environ. Microbiol.* 68, 3509–3513. doi:10.1128/AEM.68.7.3509-3513.2002.
- 579 Marshall, A., Longmore, A., Phillips, L., Tang, C., Hayden, H., Heidelberg, K., et al. (2021).
580 Nitrogen cycling in coastal sediment microbial communities with seasonally variable benthic
581 nutrient fluxes. *Aquat. Microb. Ecol.* 86, 1–19. doi:10.3354/ame01954.

- 582 Marshall, I. P. G., Ren, G., Jaussi, M., Lomstein, B. A., Jørgensen, B. B., Røy, H., et al. (2019).
583 Environmental filtering determines family-level structure of sulfate-reducing microbial communities
584 in subsurface marine sediments. *ISME J.* 13, 1920–1932. doi:10.1038/s41396-019-0387-y.
- 585 Middelburg, J. J. (1989). A simple rate model for organic matter decomposition in marine
586 sediments. *Geochim. Cosmochim. Acta* 53, 1577–1581. doi:10.1016/0016-7037(89)90239-1.
- 587 Mori, K., and Suzuki, K.-i. (2014). “The family *Thioalkalispiraceae*,” in *The prokaryotes: Gammaproteobacteria*, eds. E. Rosenberg, E. F. DeLong, S. Lory, E. Stackebrandt, and F. Thompson (Berlin, Heidelberg: Springer-Verlag), 653–658. doi:10.1007/978-3-642-38922-1_399.
- 588 Mori, K., Suzuki, K.-I., Urabe, T., Sugihara, M., Tanaka, K., Hamada, M., et al. (2011).
589 *Thiopropfundum hispidum* sp. nov., an obligately chemolithoautotrophic sulfur-oxidizing
590 gammaproteobacterium isolated from the hydrothermal field on Suiyo Seamount, and proposal
591 of *Thioalkalispiraceae* fam. nov. in the order *Chromatiales*. *Int. J. Syst. Evol. Microbiol.* 61,
592 2412–2418. doi:10.1099/ijts.0.026963-0.
- 593 Najdek, M., Korlević, M., Paliaga, P., Markovski, M., Ivančić, I., Iveša, L., et al. (2020).
594 Dynamics of environmental conditions during the decline of a *Cymodocea nodosa* meadow.
595 *Biogeosciences* 17, 3299–3315. doi:10.5194/bg-17-3299-2020.
- 596 Neuwirth, E. (2014). *RColorBrewer: ColorBrewer palettes*.
- 597 Oksanen, J., Blanchet, F. G., Friendly, M., Kindt, R., Legendre, P., McGlinn, D., et al. (2020).
598 *vegan: Community ecology package*.
- 599 Orcutt, B. N., Sylvan, J. B., Knab, N. J., and Edwards, K. J. (2011). Microbial ecology
600 of the dark ocean above, at, and below the seafloor. *Microbiol. Mol. Biol. Rev.* 75, 361–422.
601 doi:10.1128/MMBR.00039-10.

- 604 Orlando-Bonaca, M., Francé, J., Mavrič, B., Grego, M., Lipej, L., Flander-Putrl, V., et al.
605 (2015). A new index (MediSkew) for the assessment of the *Cymodocea nodosa* (Ucria) Ascherson
606 meadow's status. *Mar. Environ. Res.* 110, 132–141. doi:10.1016/j.marenvres.2015.08.009.
- 607 Orsi, W. D. (2018). Ecology and evolution of seafloor and subseafloor microbial communities.
608 *Nat. Rev. Microbiol.* 16, 671–683. doi:10.1038/s41579-018-0046-8.
- 609 Parada, A. E., Needham, D. M., and Fuhrman, J. A. (2016). Every base matters: Assessing
610 small subunit rRNA primers for marine microbiomes with mock communities, time series and
611 global field samples. *Environ. Microbiol.* 18, 1403–1414. doi:10.1111/1462-2920.13023.
- 612 Petro, C., Starnawski, P., Schramm, A., and Kjeldsen, K. (2017). Microbial community
613 assembly in marine sediments. *Aquat. Microb. Ecol.* 79, 177–195. doi:10.3354/ame01826.
- 614 Petro, C., Zäncker, B., Starnawski, P., Jochum, L. M., Ferdelman, T. G., Jørgensen, B. B., et
615 al. (2019). Marine deep biosphere microbial communities assemble in near-surface sediments in
616 Aarhus Bay. *Front. Microbiol.* 10, 758. doi:10.3389/fmicb.2019.00758.
- 617 Pfeifer, L., and Classen, B. (2020). The cell wall of seagrasses: Fascinating, peculiar and a
618 blank canvas for future research. *Front. Plant Sci.* 11, 588754. doi:10.3389/fpls.2020.588754.
- 619 Pjevac, P., Meier, D. V., Markert, S., Hentschker, C., Schweder, T., Becher, D., et al. (2018).
620 Metaproteogenomic profiling of microbial communities colonizing actively venting hydrothermal
621 chimneys. *Front. Microbiol.* 9, 680. doi:10.3389/fmicb.2018.00680.
- 622 Polymenakou, P., Bertilsson, S., Tselepidis, A., and Stephanou, E. (2005). Bacterial
623 community composition in different sediments from the Eastern Mediterranean Sea: A
624 comparison of four 16S ribosomal DNA clone libraries. *Microb. Ecol.* 50, 447–62.
625 doi:10.1007/s00248-005-0005-6.

626 Quast, C., Pruesse, E., Yilmaz, P., Gerken, J., Schweer, T., Yarza, P., et al. (2013). The SILVA
627 ribosomal RNA gene database project: Improved data processing and web-based tools. *Nucleic*
628 *Acids Res.* 41, D590–D596. doi:10.1093/nar/gks1219.

629 Rabbani, G., Yan, B. C., Lee, N. L. Y., Ooi, J. L. S., Lee, J. N., Huang, D., et al. (2021). Spatial
630 and structural factors shape seagrass-associated bacterial communities in Singapore and Peninsular
631 Malaysia. *Front. Mar. Sci.* 8, 590. doi:10.3389/fmars.2021.659180.

632 R Core Team (2020). *R: A language and environment for statistical computing*. Vienna,
633 Austria: R foundation for statistical computing.

634 Rinke, C., Rubino, F., Messer, L. F., Youssef, N., Parks, D. H., Chuvochina, M., et al. (2019).
635 A phylogenomic and ecological analysis of the globally abundant Marine Group II archaea (*Ca.*
636 *Poseidoniales* ord. nov.). *ISME J.* 13, 663–675. doi:10.1038/s41396-018-0282-y.

637 Ruiz Fernandez, J. M., Boudouresque, C., and Enríquez, S. (2009). Seagrass ecosystems and
638 Mediterranean seagrasses. *Botanica Marina* 52, 369–381. doi:10.1515/BOT.2009.058.

639 Schloss, P. D., Jenior, M. L., Koumpouras, C. C., Westcott, S. L., and Highlander, S. K. (2016).
640 Sequencing 16S rRNA gene fragments using the PacBio SMRT DNA sequencing system. *PeerJ* 4,
641 e1869. doi:10.7717/peerj.1869.

642 Schloss, P. D., Westcott, S. L., Ryabin, T., Hall, J. R., Hartmann, M., Hollister, E. B., et al.
643 (2009). Introducing mothur: Open-source, platform-independent, community-supported software
644 for describing and comparing microbial communities. *Appl. Environ. Microbiol.* 75, 7537–7541.
645 doi:10.1128/AEM.01541-09.

646 Silburn, B., Kröger, S., Parker, E. R., Sivyer, D. B., Hicks, N., Powell, C. F., et al. (2017).
647 Benthic pH gradients across a range of shelf sea sediment types linked to sediment characteristics
648 and seasonal variability. *Biogeochemistry* 135, 69–88. doi:10.1007/s10533-017-0323-z.

- 649 Smith, A. C., Kostka, J. E., Devereux, R., and Yates, D. F. (2004). Seasonal composition and
650 activity of sulfate-reducing prokaryotic communities in seagrass bed sediments. *Aquat. Microb.*
651 *Ecol.* 37, 183–195. doi:10.3354/ame037183.
- 652 Starnawski, P., Bataillon, T., Ettema, T. J. G., Jochum, L. M., Schreiber, L., Chen, X., et al.
653 (2017). Microbial community assembly and evolution in subseafloor sediment. *Proc. Natl. Acad.*
654 *Sci. U.S.A.* 114, 2940–2945. doi:10.1073/pnas.1614190114.
- 655 Sun, F., Zhang, X., Zhang, Q., Liu, F., Zhang, J., and Gong, J. (2015). Seagrass (*Zostera*
656 *marina*) colonization promotes the accumulation of diazotrophic bacteria and alters the relative
657 abundances of specific bacterial lineages involved in benthic carbon and sulfur cycling. *Appl.*
658 *Environ. Microbiol.* 81, 6901–6914. doi:10.1128/AEM.01382-15.
- 659 Sun, Y., Song, Z., Zhang, H., Liu, P., and Hu, X. (2020). Seagrass vegetation affect the
660 vertical organization of microbial communities in sediment. *Mar. Environ. Res.* 162, 105174.
661 doi:10.1016/j.marenvres.2020.105174.
- 662 Terrados, J., and Duarte, C. M. (2000). Experimental evidence of reduced particle
663 resuspension within a seagrass (*Posidonia oceanica*) meadow. *J. Exp. Mar. Biol. Ecol.* 243, 45–53.
664 doi:10.1016/S0022-0981(99)00110-0.
- 665 Thomas, F., Hehemann, J.-H., Rebuffet, E., Czjzek, M., and Michel, G. (2011).
666 Environmental and gut *Bacteroidetes*: The food connection. *Front. Microbiol.* 2, 93.
667 doi:10.3389/fmicb.2011.00093.
- 668 Torti, A., Jørgensen, B. B., and Lever, M. A. (2018). Preservation of microbial DNA in
669 marine sediments: Insights from extracellular DNA pools. *Environ. Microbiol.* 20, 4526–4542.
670 doi:10.1111/1462-2920.14401.

- 671 Tuya, F., Ribeiro-Leite, L., Arto-Cuesta, N., Coca, J., Haroun, R., and Espino, F. (2014).
- 672 Decadal changes in the structure of *Cymodocea nodosa* seagrass meadows: Natural vs. human
673 influences. *Estuar. Coast. Shelf Sci.* 137, 41–49. doi:10.1016/j.ecss.2013.11.026.
- 674 van Katwijk, M. M., Bos, A. R., Hermus, D. C. R., and Suykerbuyk, W. (2010). Sediment
675 modification by seagrass beds: Muddification and sandification induced by plant cover and
676 environmental conditions. *Estuar. Coast. Shelf Sci.* 89, 175–181. doi:10.1016/j.ecss.2010.06.008.
- 677 Walsh, E. A., Kirkpatrick, J. B., Rutherford, S. D., Smith, D. C., Sogin, M., and D'Hondt, S.
678 (2016). Bacterial diversity and community composition from seafloor to subseafloor. *ISME J.* 10,
679 979–989. doi:10.1038/ismej.2015.175.
- 680 Watanabe, M., Fukui, M., Galushko, A., and Kuever, J. (2020). “*Desulfosarcina*,” in *Bergey's*
681 *manual of systematics of Archaea and Bacteria*, ed. W. B. Whitman (online: John Wiley & Sons, in
682 association with Bergey's manual trust), 1–6. doi:10.1002/9781118960608.gbm01020.pub2.
- 683 Wickham, H., Averick, M., Bryan, J., Chang, W., McGowan, L. D., François, R., et al. (2019).
- 684 Welcome to the tidyverse. *J. Open Source Softw.* 4, 1686. doi:10.21105/joss.01686.
- 685 Wilke, C. O. (2020). *Cowplot: Streamlined plot theme and plot annotations for 'ggplot2'*.
- 686 Xie, Y. (2014). “knitr: A comprehensive tool for reproducible research in R,” in *Implementing*
687 *reproducible computational research*, eds. V. Stodden, F. Leisch, and R. D. Peng (New York:
688 Chapman and Hall/CRC), 3–32.
- 689 Xie, Y. (2015). *Dynamic documents with R and knitr*. 2nd ed. Boca Raton, Florida: Chapman
690 and Hall/CRC.
- 691 Xie, Y. (2019). TinyTeX: A lightweight, cross-platform, and easy-to-maintain LaTeX
692 distribution based on TeX Live. *TUGboat* 40, 30–32.
- 693 Xie, Y. (2021a). *knitr: A general-purpose package for dynamic report generation in R*.

- 694 Xie, Y. (2021b). *tinytex: Helper functions to install and maintain 'TeX Live', and compile*
695 *'LaTeX' documents.*
- 696 Xie, Y., Allaire, J. J., and Grolemund, G. (2018). *R Markdown: The definitive guide*. 1st ed.
697 Boca Raton, Florida: Chapman and Hall/CRC.
- 698 Xie, Y., Deriveux, C., and Riederer, E. (2020). *R Markdown cookbook*. 1st ed. Boca Raton,
699 Florida: Chapman and Hall/CRC.
- 700 Yilmaz, P., Parfrey, L. W., Yarza, P., Gerken, J., Pruesse, E., Quast, C., et al. (2014). The
701 SILVA and “All-species Living Tree Project (LTP)” taxonomic frameworks. *Nucleic Acids Res.* 42,
702 D643–D648. doi:10.1093/nar/gkt1209.
- 703 Zhang, X., Liu, S., Jiang, Z., Wu, Y., and Huang, X. (2022). Gradient of microbial
704 communities around seagrass roots was mediated by sediment grain size. *Ecosphere* 13, e3942.
705 doi:10.1002/ecs2.3942.
- 706 Zhang, X., Zhao, C., Yu, S., Jiang, Z., Liu, S., Wu, Y., et al. (2020). Rhizosphere microbial
707 community structure is selected by habitat but not plant species in two tropical seagrass beds. *Front.*
708 *Microbiol.* 11, 161. doi:10.3389/fmicb.2020.00161.
- 709 Zheng, P., Wang, C., Zhang, X., and Gong, J. (2019). Community structure and abundance of
710 archaea in a *Zostera marina* meadow: A comparison between seagrass-colonized and bare sediment
711 sites. *Archaea* 2019, e5108012. doi:10.1155/2019/5108012.
- 712 Zhou, J., Bruns, M. A., and Tiedje, J. M. (1996). DNA recovery from soils of diverse
713 composition. *Appl. Environ. Microbiol.* 62, 316–322. doi:10.1128/aem.62.2.316-322.1996.
- 714 Zhu, H. (2021). *kableExtra: Construct complex table with 'kable' and pipe syntax*.

715 **Figure legends**

716 **Figure 1.** Location of the vegetated (declining *Cymodocea nodosa* meadow) and nonvegetated site
717 in the Bay of Saline, northern Adriatic Sea, together with visual representations of vegetated and
718 nonvegetated sediment cores (© OpenStreetMap contributors, www.openstreetmap.org/copyright).

719 **Figure 2.** The observed number of OTUs, Chao1, ACE, exponential of the Shannon diversity
720 index, and Inverse Simpson diversity index of sediment microbial communities sampled in different
721 sediment layers of the vegetated and nonvegetated site in the Bay of Saline.

722 **Figure 3.** Principal Coordinates Analysis (PCoA) of Bray-Curtis dissimilarities based on OTU
723 abundances of sediment microbial communities sampled in the Bay of Saline. Samples from
724 different sites are labelled with different symbols while samples from different sediment layers
725 are indicated by colour. The proportion of explained variation by each axis is shown on the
726 corresponding axis in parentheses.

727 **Figure 4.** Principal Coordinates Analyses (PCoA) of Bray-Curtis dissimilarities based on OTU
728 abundances of sediment microbial communities, of all and individual sediment layers, sampled at
729 the vegetated and nonvegetated site in the Bay of Saline. The proportion of explained variation by
730 each axis is shown on the corresponding axis in parentheses.

731 **Figure 5.** Taxonomic classification and relative contribution of the most abundant bacterial and
732 archaeal ($\geq 3\%$) sequences in sediment communities sampled at the vegetated and nonvegetated
733 site in the Bay of Saline. NR – sequences without known relatives

734 **Figure 6.** Taxonomic classification and relative contribution of the most abundant ($\geq 2\%$) taxonomic
735 groups within *Desulfobacterota*, *Gammaproteobacteria*, and *Bacteroidota* in sediment communities
736 sampled at the vegetated and nonvegetated site in the Bay of Saline. NR – sequences without known
737 relatives

738 **Figure 7.** Taxonomic classification and relative contribution of the most abundant ($\geq 1\%$) taxonomic
739 groups within *Chloroflexi*, *Planctomycetota*, and *Campylobacterota* in sediment communities
740 sampled at the vegetated and nonvegetated site in the Bay of Saline. NR – sequences without known
741 relatives

742 **Figures**

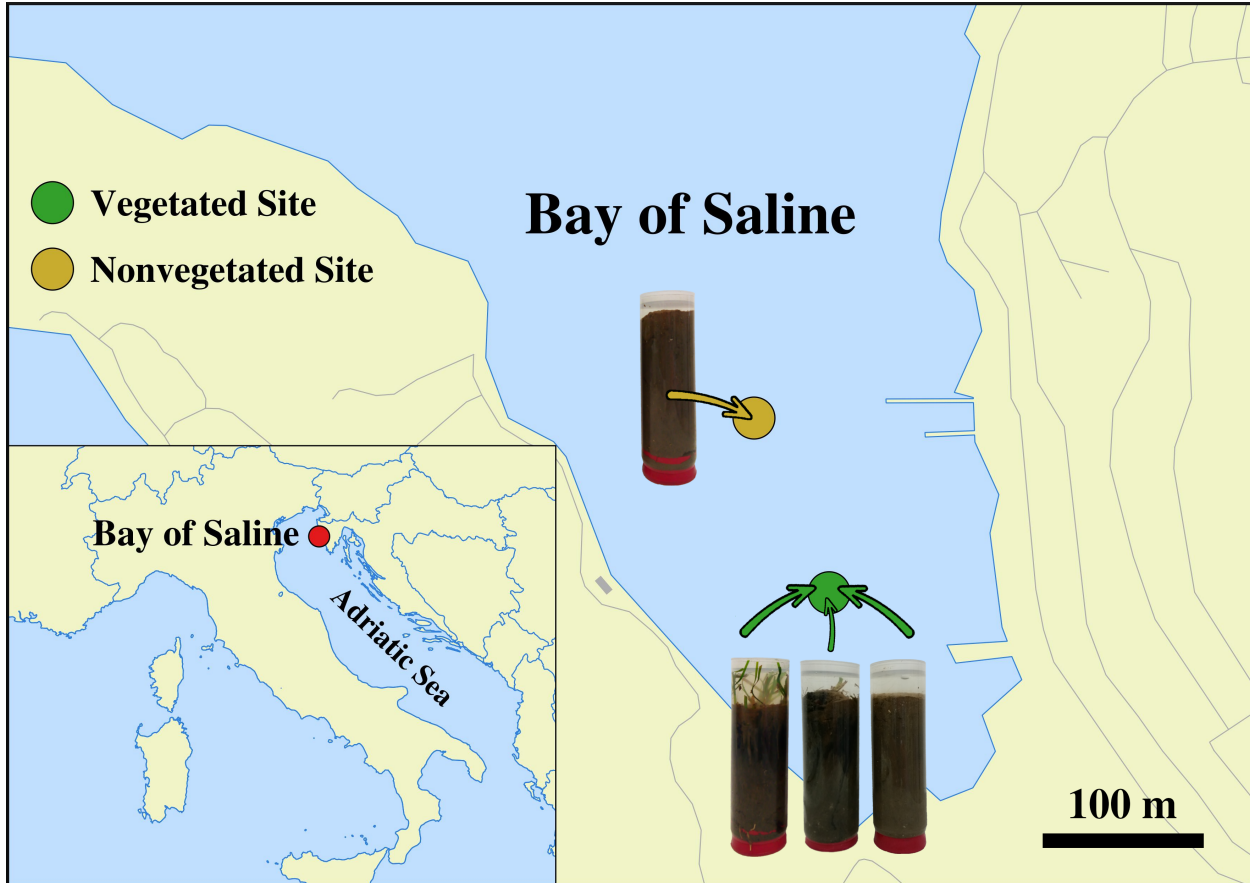


Figure 1. Location of the vegetated (declining *Cymodocea nodosa* meadow) and nonvegetated site in the Bay of Saline, northern Adriatic Sea, together with visual representations of vegetated and nonvegetated sediment cores (© OpenStreetMap contributors, www.openstreetmap.org/copyright).

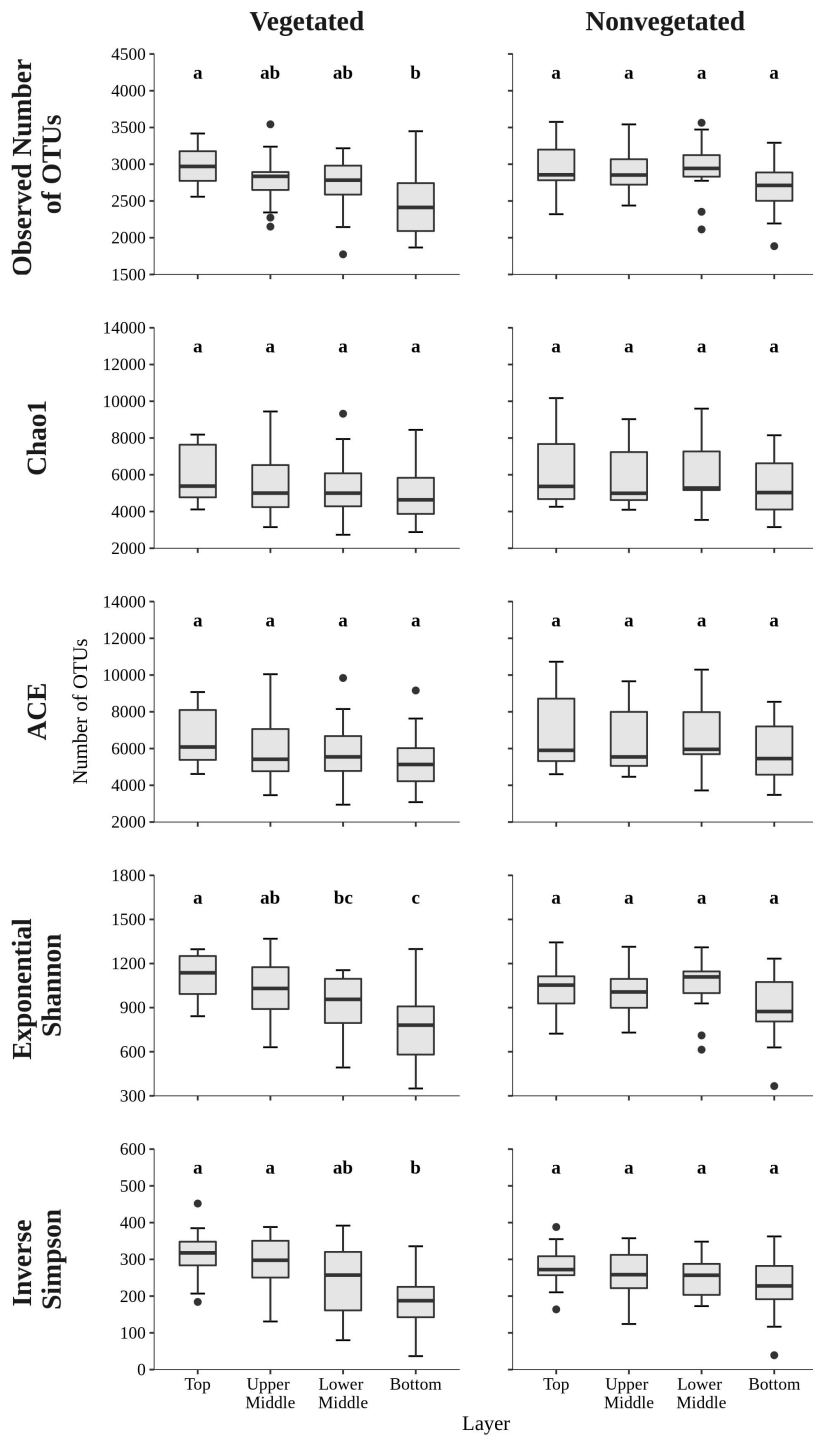


Figure 2. The observed number of OTUs, Chao1, ACE, exponential of the Shannon diversity index, and Inverse Simpson diversity index of sediment microbial communities sampled in different sediment layers of the vegetated and nonvegetated site in the Bay of Saline.

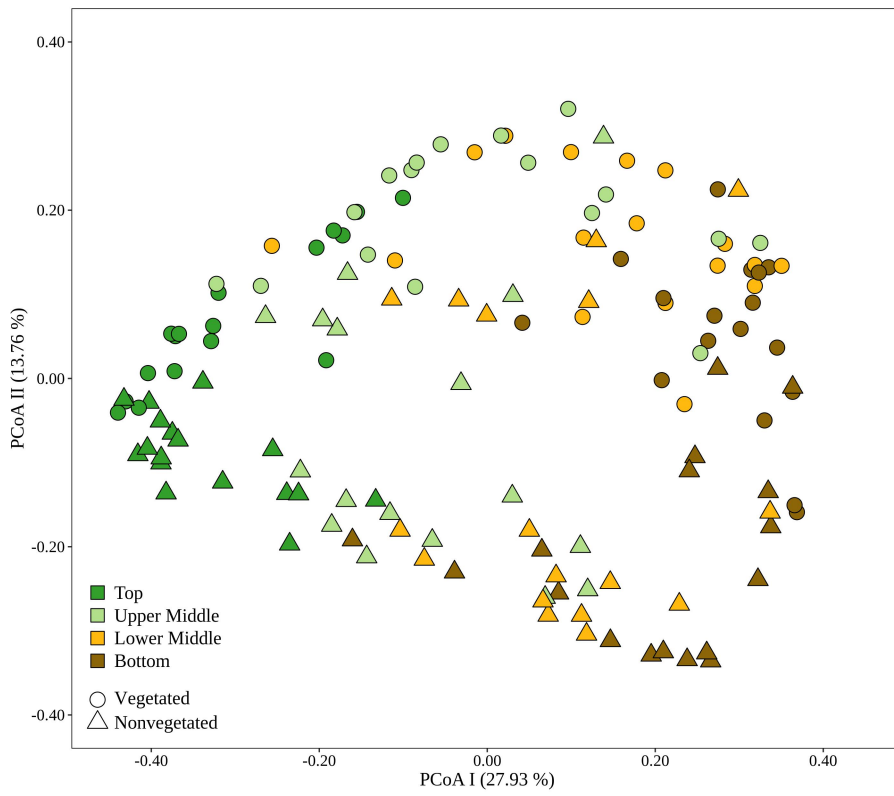


Figure 3. Principal Coordinates Analysis (PCoA) of Bray-Curtis dissimilarities based on OTU abundances of sediment microbial communities sampled in the Bay of Saline. Samples from different sites are labelled with different symbols while samples from different sediment layers are indicated by colour. The proportion of explained variation by each axis is shown on the corresponding axis in parentheses.

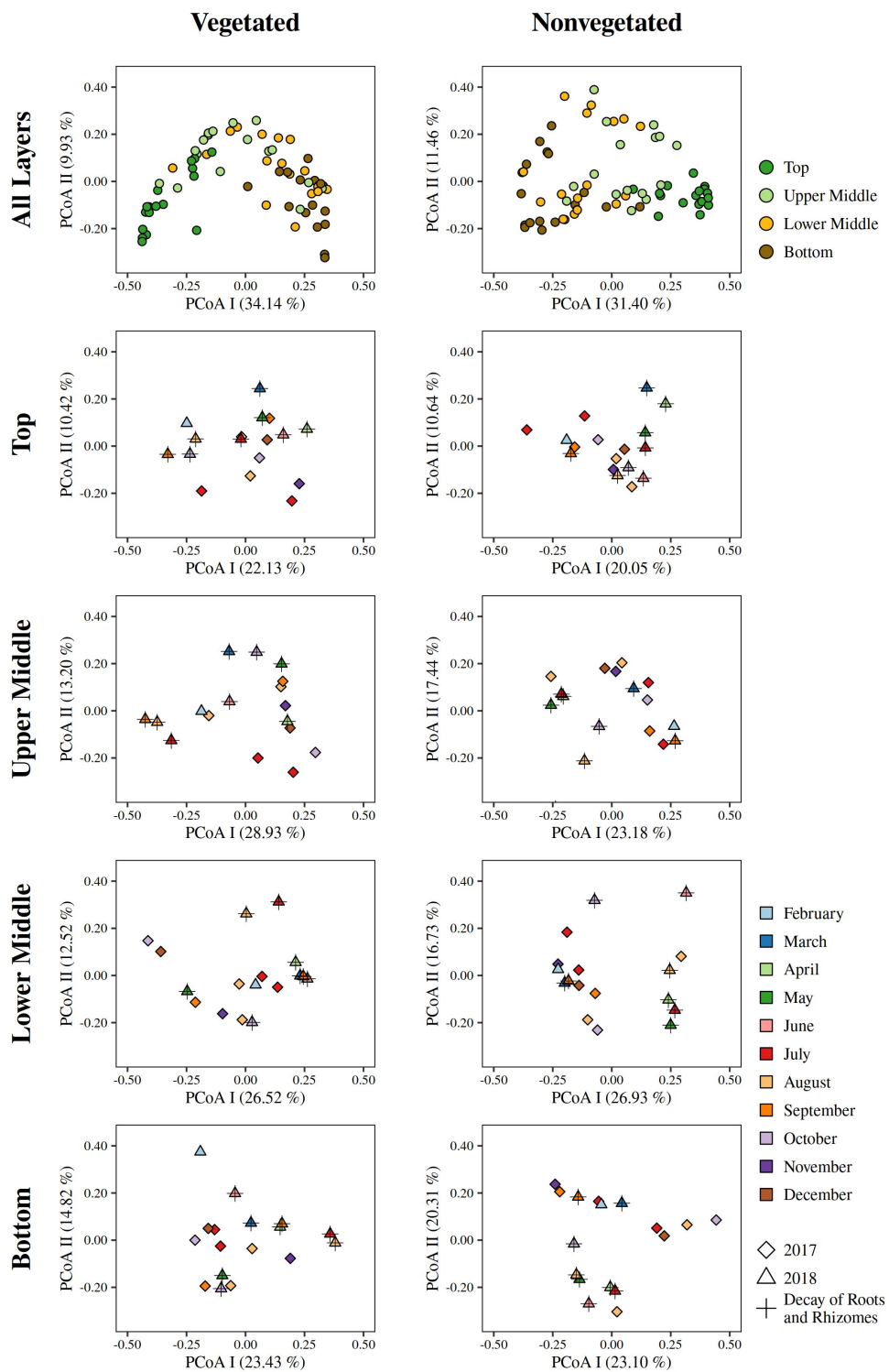


Figure 4. Principal Coordinates Analyses (PCoA) of Bray-Curtis dissimilarities based on OTU abundances of sediment microbial communities, of all and individual sediment layers, sampled at the vegetated and nonvegetated site in the Bay of Saline. The proportion of explained variation by each axis is shown on the corresponding axis in parentheses.

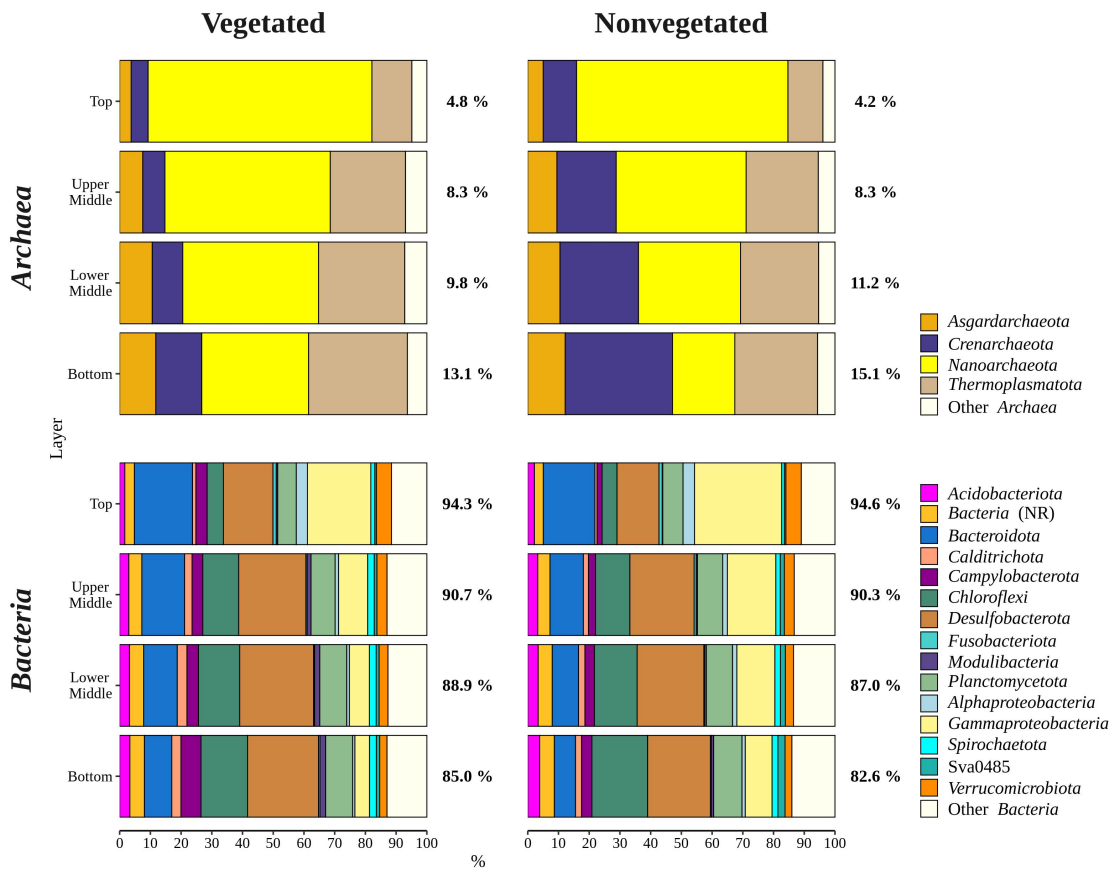


Figure 5. Taxonomic classification and relative contribution of the most abundant bacterial and archaeal ($\geq 3\%$) sequences in sediment communities sampled at the vegetated and nonvegetated site in the Bay of Saline. NR – sequences without known relatives

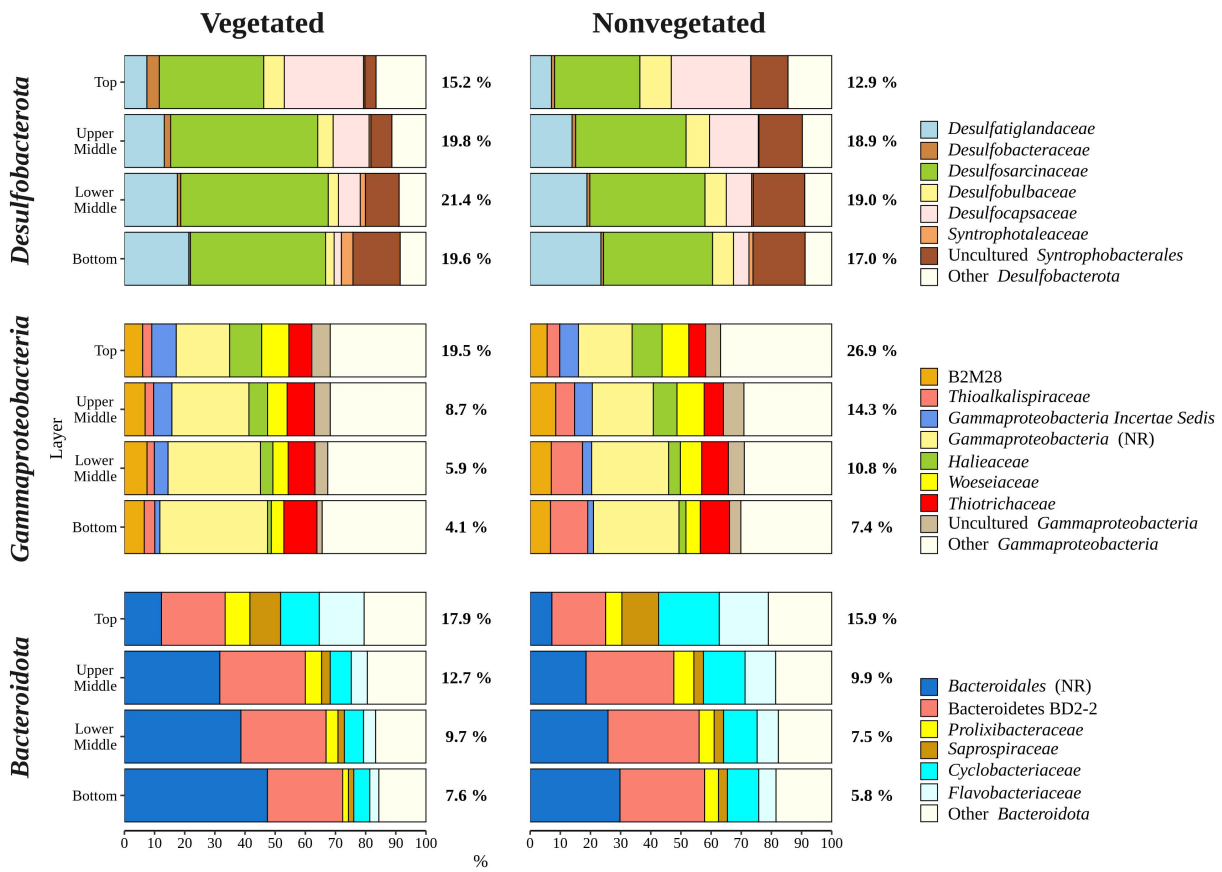


Figure 6. Taxonomic classification and relative contribution of the most abundant ($\geq 2\%$) taxonomic groups within *Desulfobacterota*, *Gammaproteobacteria*, and *Bacteroidota* in sediment communities sampled at the vegetated and nonvegetated site in the Bay of Saline. NR – sequences without known relatives

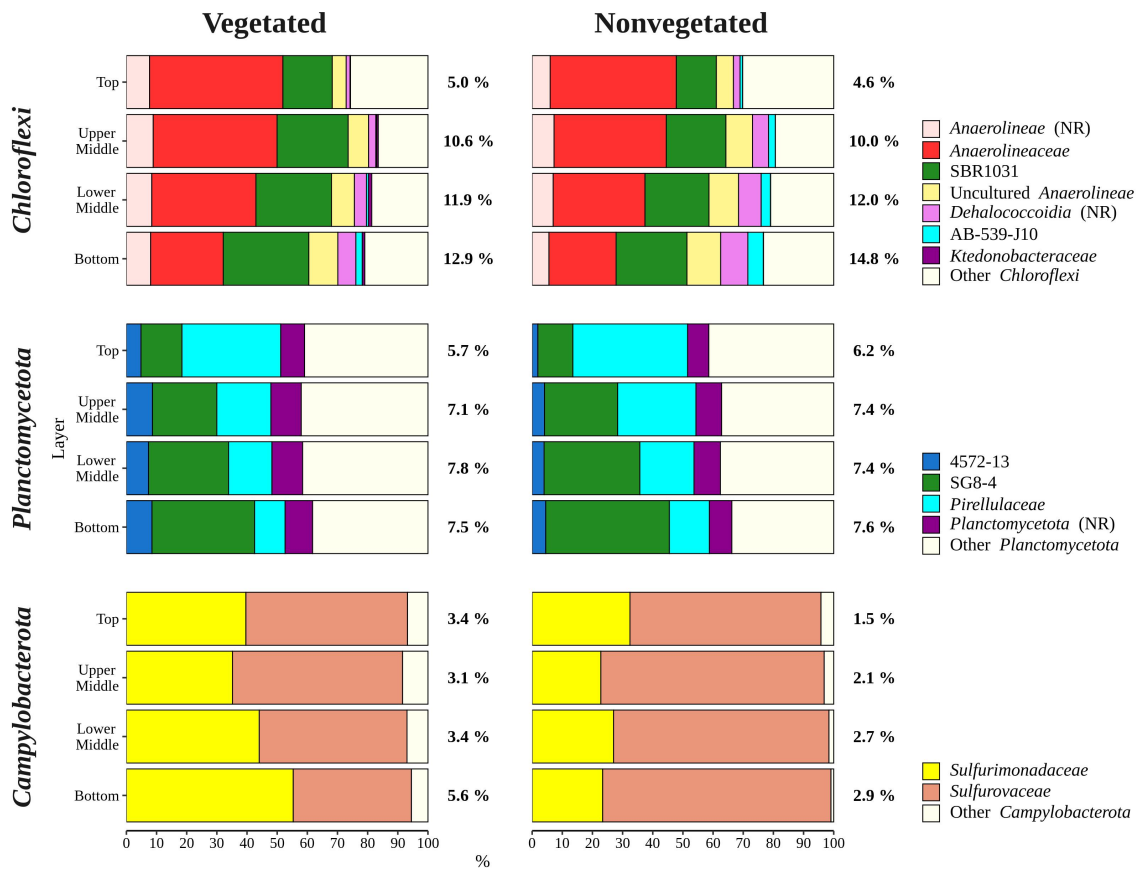


Figure 7. Taxonomic classification and relative contribution of the most abundant ($\geq 1\%$) taxonomic groups within *Chloroflexi*, *Planctomycetota*, and *Campylobacterota* in sediment communities sampled at the vegetated and nonvegetated site in the Bay of Saline. NR – sequences without known relatives